

DFTB1 and DFTB2 Based Real-Time Flipping Motion Studies of Central Phenylene Rotator of Crystalline Siloxaalkane Molecular Gyroscope

Prof. Dr. Anant Babu Marahatta^{1,*}

¹Engineering Chemistry and Applied Science Research Unit, Department of Civil, Computer and Electronics Engineering, Kathford Int'l College of Engineering and Management (Affiliated to Tribhuvan University), Kathford Int'l Education & Research Foundation, Lalitpur, Nepal

*Corresponding author: abmarahatta@gmail.com/anant.marahatta@kathford.edu.np



Abstract – Despite adopting *ab initio* functionalities comprising mathematical formulations and many unique complex computational features, the density-functional based tight-binding (DFTB) scheme presents itself as the standalone, versatile, and efficient quantum mechanical application. The recognizably low-cost, & extremely faster MD simulation parser codes of it run under the DFTB⁺ atomic simulation environment interface plus the noticeably methodical long ranged molecular interactions addressing 'non-self-consistent-charge' (DFTB1) & 'self-consistent-charge' (DFTB2) formulations adds a substantial value to its rational applications. Herewith, both the DFTB2/ & DFTB1/ MD simulation schemes are employed separately to simulate the siloxaalkane molecular gyroscope under crystalline condition with and without 'dispersion energy corrections' features at wide temperature regimes & the experimentally observed facile flipping motions of its central phenylene rotator are confirmed theoretically in real-time scales. The concerned rotary trajectories depict that: (a) at $800\text{ K} \leq T \leq 1200\text{ K}$, the rotator exhibits 1π inversions & frequent flipping motions easily with sub-picoseconds to picoseconds lifetimes; (b) at $T = 600\text{ K}$, the rotator flips between its stable positions at the intervals of several tens of picoseconds; but (c) at $T = 300\text{ K}$, the rotator flips more demonstratively with longer lifespans only after addressing the dispersion energies in DFTB2 scheme. Additionally, the flipping rates of the rotator; $\kappa_1 = 0.018\text{ ps}^{-1}$ & $\kappa_2 = 0.021\text{ ps}^{-1}$ predicted at $T = 800\text{ K}$ & 1200 K respectively are retarded to 0.009 ps^{-1} & 0.013 ps^{-1} , and the flipping barrier estimated by using κ_1 & κ_2 as $E_{a1} = 0.66\text{ kcal/mol}$ is increased to $E_{a2} = 1.84\text{ kcal/mol}$ after treating dispersion energies; the quite consistent values to those retrieved from the respectively derived potential energy surface ($E_{a1} = 0.70\text{ kcal/mol}$ & $E_{a2} = 1.2\text{ kcal/mol}$). These quantitative results illuminate that the DFTB2/MD simulation scheme is more demandable than the DFTB1/MD especially for simulating crystalline molecular assembly.

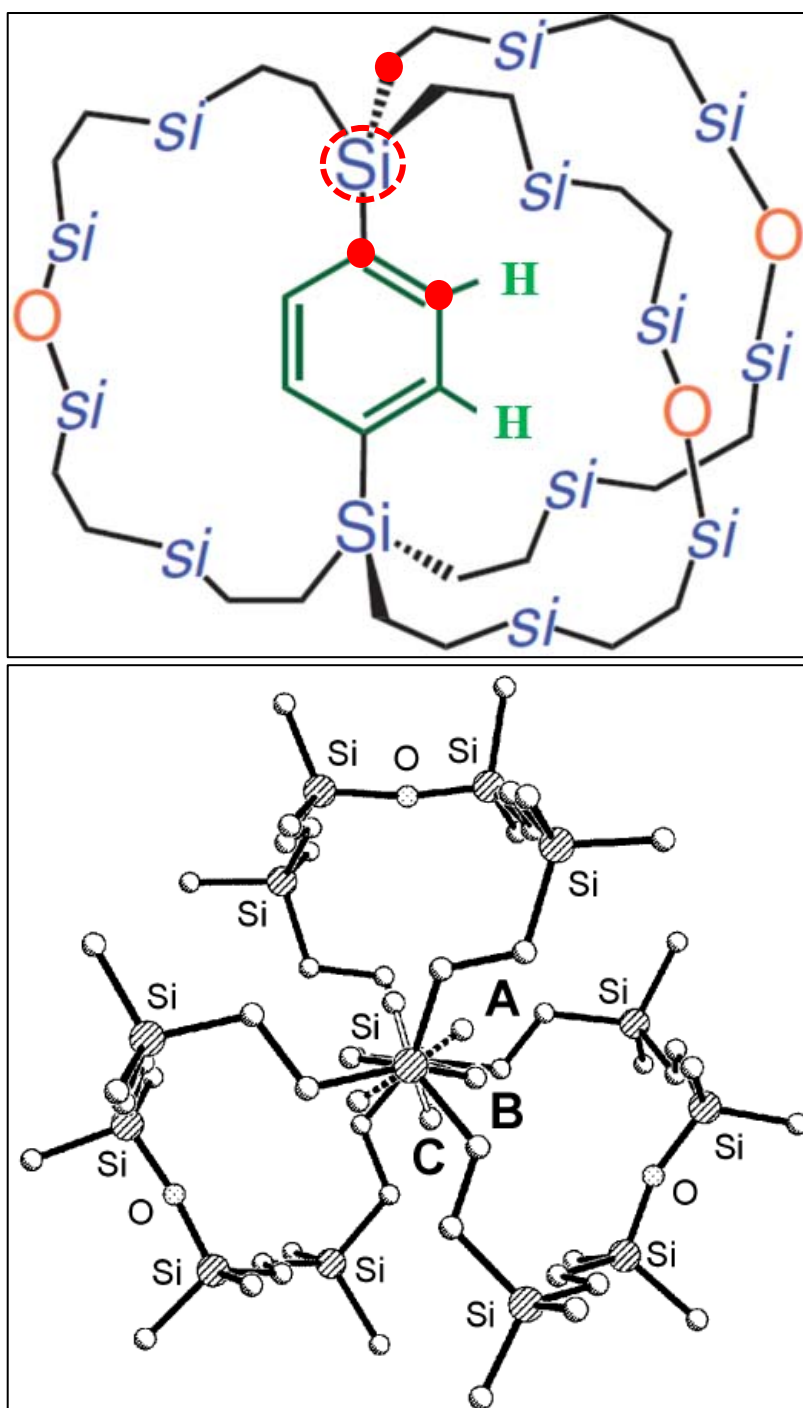
Keywords – MD Simulation, Nanotechnology, Flipping Motions/Rates/Barriers, Arrhenius Equation.

I. INTRODUCTION

In the lately evolved and recently emerged scientific paradigms, and many other state-of-art computational/theoretical interpretations and analyses, the performances of quantum mechanical models/theoretical schemes equipped with the specific mathematical algorithms & parametrizations and their formulations—compatible three dimensional visualizations & modeling tools are regarded as exceptional. The *ab initio* functionalities comprising mathematical formulations founded density-functional based tight-binding (DFTB) scheme is one of them whose profound theoretical features extended mainly to address the giant crystalline macrocyclic molecular systems plus efficient yet precise computing abilities even under crystalline condition (periodic boundary condition (hereafter, PBC)) with and without "dispersion energy corrections" have made itself to stand as a reputable theoretical scheme [1–7]. More particularly, its python moduled computational parser codes, solid-state centric theoretical features that are not yet implemented fully in other quantum mechanical schemes, DFT based yet one or two orders of magnitude faster, low-cost, and users' friendly simulation package, quantum simulation tools and techniques, *Gaussian-External* methodology executable coding and externally assessable method via the 'external program' feature of the *Gaussian*, integrative quantum mechanical approximations into many other computational schemes [1–5], extremely methodical & probably the most efficient and versatile approach to evaluate both the homo- & hetero- atomic giant crystalline and non-crystalline molecular assemblies with wide ranged atomic constituents, etc. [8, 9] features act as a stepping-stone to promote itself extensively. It usually operates all these quantum mechanical features through either the "non-self-consistent-charge NCC" (hereafter, DFTB1) approach or the "self-consistent-charge SCC" (hereafter, DFTB2). The concerned computational parser codes designed for both of them are "open-source" type, and are directly implementable under the both crystalline and non-crystalline conditions as per the needs of the users. In terms of their in-built quantum mechanical parametrizations; (a) former approach is a traditional NCC tight binding with standard zeroth-order expansions of the Kohn–Sham total energy in DFT with respect to charge density fluctuations where the Eigenvalue of the Hamiltonian operator is a result of the non-iterative computations, but the latter is an iterative SCC method with standard second-order expansions, (b) former cannot incorporate the Mulliken charges fully, and hence, derives relatively less transparent & readily unsolvable mathematical expressions unlike to that of the latter, (c) former is less relevant to undertake "dispersion energy corrections" algorithms (in this case, Slater–Kirkwood model, and Slater–Koster files (SK-files)) under PBC but the latter suits for the same as it computes SCC procedure based nuclear forces and treats the heteroatomic charge distribution (point charges) uniquely [1–4]. Therefore, the specific results produced by both of them are even though quite agreeable and are as standard as DFT (6–31G (d)) [8], and other high-level *ab initio* & first principle methods plus semi-empirical AM1 and PM3 [10] levels, their performances are already evaluated as distinctly varied more especially while employing them under PBC with and without Slater–Kirkwood dispersion model [6–8].

Besides their valuable yet efficient low energy electronic structures searching iterative computational procedures, and the related quantum mechanical processing, the dynamics simulations assessing abilities of them for the complex crystalline molecular assembly under the DFTB⁺ open-source codes package add substantial values to their explicit demands more especially in the field of crystalline nanomaterials and amphidynamic molecular assemblies [9,11]. Both of them are well recognizable in terms of implementing molecular dynamics (hereafter, MD) simulations hosting mathematical formulations genuinely, and of running atomistic simulations efficiently under the python moduled DFTB⁺ atomic simulation environment (ASE) interface by accessing the different levels of quantum mechanical theories including DFT parametrizations & other classical potentials [11,12]. The underlying facts behind their nominations as one of the most versatile quantum mechanical simulation packages are none other than their specifically derived mathematical credentials suitable to carry out very faithful MD simulations such as nuclear forces, equilibrium geometry, programmatic pathways of accessing local properties targeted to look after the global ones, band-structure associated energy terms responsible to address more especially the long-ranged van der Waals type nonbonding interactions, short-ranged energetics curing transferable formulations, etc. More apparently, the Slater–Kirkwood dispersion model and SK-files compatible MD formulations of the DFTB2 under PBC offer relatively far better and more quantitative theoretical means over DFTB1 for investigating the dynamics of complex macrocyclic crystalline molecular systems [11, 12]. In this study, the MD simulations formulations of the DFTB2 and DFTB1 under PBC with and without "dispersion energy corrections" are employed, and the X-ray observed flipping motions of the phenylene rotator of crystalline siloxaalkane molecular gyroscope (Scheme 1(a)) are inquired in real-time scales at wide ranged kinetic temperatures T.

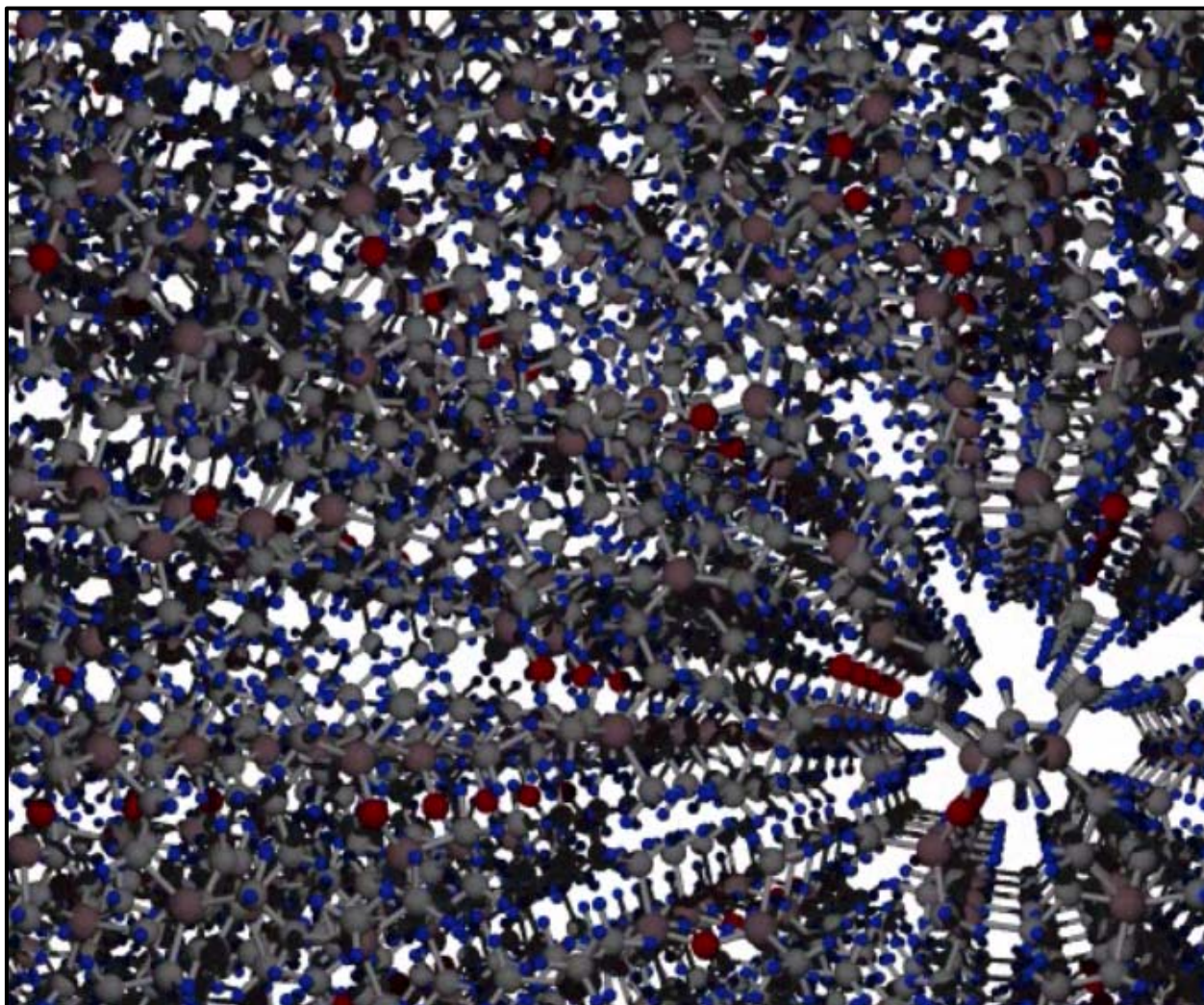
According to the experimental observations, each siloxaalkane molecular gyroscope of its crystalline molecular arrays exhibits macroscopic gyroscope like functions at ambient temperatures range (223 K–303 K) [13]: the central phenylene rotator flips along the Si–C axial bond spin axis in between the three stable positions A, B, and C by conserving its internal volume (Scheme 1(b)), and the peripheral –Si– & –Si–O–Si– made siloxaalkane arms remain fully immobile & static throughout its complete 2π rotation. The collective rotations of all the molecular gyroscopes present in the crystalline network (Scheme 2) are expected to deliver many promising functionalizable physicochemical properties: the externally controllable flipping motion after inserting dipolar electronegative groups into the ortho– and meta– positions of the phenylene rotator [14]; the optical anisotropy marking dichroism and birefringence phenomena [15]; the microviscosity probing molecular rotors [16], etc. The detailed theoretical investigations focusing on searching the lowest energy equilibrium structure among A, B, & C and their explicit energetics plus stable electronic structures, deriving the consequences of structural deformations and siloxaalkane arms' elongations, deducing the increment or decrement of the free–volume unit around the rotating segment while the peripheral arms move outward (ballooning) or inward (dwindling), determining the rotational potential energy surfaces (hereafter, PESs) displaying flipping barriers E_a and specific locations of the local/global minima quantitatively, etc. are already performed by the present author and his collaborators [17–21]. Therewith, both the DFTB1 and DFTB2 methods under PBC with and without "dispersion energy corrections" were employed explicitly. Additionally, the rotary dynamics and the real–time flipping motions of the phenylene rotator at kinetic temperature regimes $T = 1200$ K, 800 K, 600 K, and 300 K were also reported by the same author elsewhere [17], but the method applied was only the DFTB1+PBC scheme. The main point to be highlighted herewith is that the "DFTB2+PBC+dispersion energy corrections" derived rotational PES was non-duplicated to that of the "DFTB1+PBC", and the barrier heights E_a (former: $E_{a1} = 1.15$ kcal/mol; latter: $E_{a2} = 0.72$ kcal/mol) computed by them were also distinctly varied yet the former one was thematically more accurate in magnitudes. Even the positions of the global and local minima A, B, & C, and their 1π –flipped degenerate equilibrium structures retrieved from the former derived PES were not harmonized fully with those of the latter [17]. In order to validate these rotary parameters to those derived from the MD simulations, the proper quantum mechanical treatments of the dispersion type van der Waals intra– (interactions between the rotator and stator) and inter– (interactions between the periodically arranged molecules) molecular interactions via the Slater– Kirkwood model implemented DFTB2/MD scheme is mandatory. The MD simulation based



Scheme 1. (a) A macrocage molecular model of the crystalline siloxaalkane molecular gyroscope, and its (b) three stable positions A, B, and C of the central phenylene rotator at 303 K. They are reproduced from ref [8] and [9] respectively for demonstrating closed structural topology and X-ray observed flipping positions respectively. The two methyl (CH_3) groups attached to each Si atom of each siloxaalkane arm are omitted for clarity. The dihedral angle used to specify the rotary position of the phenylene rotator is defined by the atoms encircled with red colored spheroids.

rotary dynamics results produced after this rigorous addressing of the solid state features at different kinetic temperature regimes

would definitely be more accurate, practically reliable, and realistically convincible. In the periphery of the same, the main objective of this study is set as to assess the performance of DFTB1/ and DFTB2/ MD schemes in order to reveal the real-time flipping dynamics of the phenylene rotator of the siloxaalkane molecular gyroscope under a complete crystalline condition which eventually be highly useful for understanding (a) functionalizing principles of the amphidynamic nanomaterials, (b) typical working and

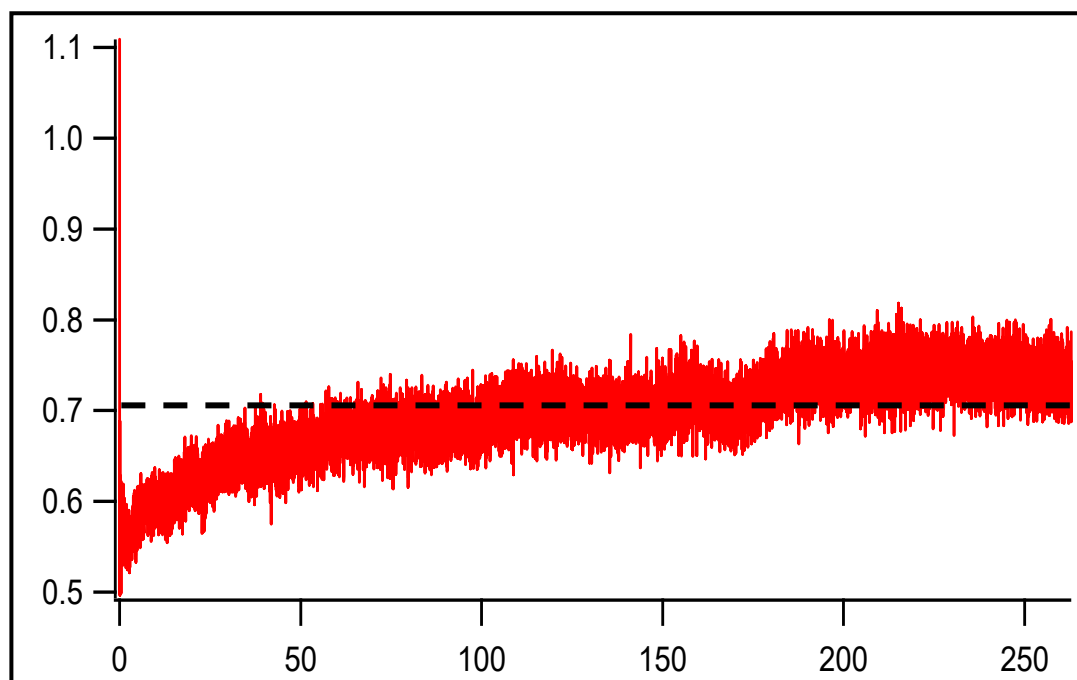


Scheme 2. A *GaussView* rendered snapshot of the periodically arranged molecular arrays of the crystalline molecular gyroscope (Scheme 1(b)). It was captured at the timescale of 1.5 ps while the DFTB2/MD simulation trajectory at $T = 1200$ K was on the fly. The 2.2 ps long movie of it are available as a supplementary material. One may access it to visualize the individual molecular motion in the crystalline environment in real-time scales.

operational mechanisms of the molecular rotor under crystalline environment, (c) macroscopic gyroscope like functions of the molecular gyroscope quantitatively, (d) tentative lifespans of the rotator at each of its stable positions, and the associated picosecond rotary dynamics at variable temperatures T , etc. Moreover, this study is focused to illuminate the effects of "dispersion energy corrections" in flipping dynamics of the rotator, and to underscore its needfulness of proper addressing while the computational simulations under the crystalline environment are on the fly. Apart from all the rotary dynamics attributes, this work offers an analogy and disagreement between the workings of DFTB1/MD and those of DFTB2/MD, and presents the leading roles of the latter with incredible quantitative justifications. This research paper is structured as: in section 2; Computational Details, in section 3; Results and Discussions, in section 4; Summary and Conclusions.

II. COMPUTATIONAL DETAILS

Out of the three experimentally observed stable positions A, B, and C of the crystalline siloxaalkane molecular gyroscope with the respective occupancy factors 0.25, 0.50, and 0.25, the Cartesian atomic coordinates of the unit-cell of the most stable structure B (phenylene position B) were taken here as a trial structure (unit-cell). The required crystallographic information such as crystal lattice, unit-cell parameters (edges of the unit-cell (lattice vectors) a , b , & c , and the angles between them α , β , & γ), etc. were extracted from the *.cif* extended files with Mercury crystallographic software tools [22]. Prior to use these unit-cell atomic coordinates directly in MD simulation input files, they were fully optimized by the both DFTB2 and DFTB1 under PBC with and without "dispersion energy corrections", and the respectively produced equilibrium nuclear positions of each atom were used there. In either of the DFTB1+PBC/ and DFTB2+PBC+ "dispersion energy corrections"/ MD methods, the initial velocities of every atomic nuclei of the unit-cell were mentioned at random so that the quantum mechanical requirements are met effectively for satisfying the mean kinetic temperature; the velocity Verlet algorithm [23] driver was programmatically called to execute the velocity Verlet dynamics for the sake of propagating atomic motions: the velocities and positions of each & every atomic nuclei of the unit-cell were determined at each MD step while the simulations trajectories were on the fly; and the time increment of each MD step and the total time duration for the entire MD run were set as 0.2 fs and 300 ps respectively. However, being the latter simulation scheme computationally very expensive and time consuming due to the charge polarization and van der Waals interactions addressing Slater–Kirkwood model adopted parser codes than that of the former, the concerned trajectories for them were forced to terminate at the reasonable simulation time scale of ~ 120 ps and ~ 300 ps respectively. Both of these simulation procedures were carried out at constant energy without any thermostating and barostating parameters so that the typical NVE ensemble was achieved throughout the entire simulations at each specific kinetic temperature T (energy) (in this case, $T = 1200$ K, 800 K, 600 K, and 300 K). In each case, no change in number of moles (N), volume (V), and energy (E) of the simulating system was ensured along with the total conservation of the net sum of kinetic energy of each simulating molecule present in the entire NVE crystalline ensemble (a representative energy profile diagram as a function of time sketched for the simulation run at $T = 300$ K is shown in Scheme 3). The common computational parser coding tags were called for operating each of these methods individually such as (a) 'MovedAtoms = 1:-1' was used to select all the atomic nuclei of the input file between start & end, and to allow all of them to move during the entire MD runs; (b) 'OutputPrefix' was called to prefix the geometry files of each MD run; (c) 'MDRestartFrequency' was set to ensure that every current nuclear positions (geometry) and velocities are written to the XYZ format geometry file; (d) 'ConvergentForcesOnly' was implemented to control the prematurely stopped dynamics; (e) the effective temperature T , defined as a mean kinetic temperature of the ensemble, etc., as mentioned in the DFTB⁺ manual [24]. The required



Scheme 3. The DFTB2 derived net kinetic energy of the simulating molecular gyroscopes present in the NVE crystalline ensemble at kinetic temperature $T = 300$ K is conserved well as a function of the simulation timescale.

dihedral angle ϕ of the phenylene rotator (the complete definition of ϕ is given in Fig. 1(a)) against its static siloxaalkane arm was computed for each MD step geometry (XYZ format) of each method at each specific kinetic temperature T , and the temporal behavior of its rotational motion was studied in real-time scales. Based on the size of the molecular ensemble and the unit-cell (number of molecules (number of atoms/molecule = 195) $Z = 2$) of the present crystalline siloxaalkane molecular gyroscope plus the available computational resources accessible directly to the present author, it was impracticable to run many MD trajectories required for taking their average ensemble. Therefore, only the few trajectories with dissimilar initial velocities at each kinetic temperature T were run, and the temperature dependence rotary dynamics was analyzed.

III. RESULTS AND DISCUSSIONS

3.1 Rotary Dynamics Associated Datasets of the Phenylene Rotator

As mentioned in the experimentally (*Expt.*) observed and theoretically (*Th.*) optimized unit-cell electronic structures and molecular energetics of the crystalline siloxaalkane molecular gyroscope based research articles published by the present author and his collaborators elsewhere [13,17, 20, 21], the three stable positions of its phenylene rotator A, B, and C (or the three stable structures A, B, and C of the unit-cell with dissimilarly aligned phenylene rotators having distinctly varied dihedral angles ϕ) located inside the cage of the static siloxaalkane spokes can be marked clearly by their respective dihedral angles ϕ measured in respect to the stationary peripheral siloxaalkane arm: $\phi = 0.19\pi$ (*Expt.*) & 0.01π (*Th.*) for position A; $\phi = 0.55\pi$ (*Expt.*) & 0.35π (*Th.*) for position B; and $\phi = 0.78\pi$ (*Expt.*) & 0.76π (*Th.*) for position C. Therewith, all these rotary stable positions of the phenylene rotator and their corresponding 1π -flipped degenerate locations respectively denoted by A', B', and C' plus the respective stable unit-cell structures are reported to be converged at slightly different ϕ values as summarized in Table 1 while searching them quantum mechanically through the PES scanning technique of the *Gaussian* package linked externally to the DFTB2 or DFTB1 methods explicitly under PBC with and without "dispersion energy corrections" (*Gaussian-External* methodology) [17]. Accordingly, the dissimilar magnitudes of the energy barriers E_a (kcal/mol) required to be crossed by the central phenylene rotator while flipping in between A, B, and C, (such as C→B, B→A, etc.) and their corresponding 1π -flipped positions A', B', and C' are

also underscored while switching the theoretical method from DFTB1 to DFTB2 (Table 2). Along with this, the pronounced quantitative differences in the flipping barriers E_a after implementing van der Waals "dispersion energy corrections" algorithm (in this case, Slater– Kirkwood model) through the DFTB2 scheme are also equally stressed. Likewise, the irreproducibility of the free–volume unit (\AA) available around the central phenylene rotator (Table 2) that actually determines whether the rotator is allowed to rotate facilely with bearing very nominal steric hindrance originated from the surrounding spokes or is prevented for exhibiting $1\pi/2\pi$ type full rotations after addressing the intra– and inter– molecular van der Waals interactions exist predominately in present crystalline molecular gyroscope is primarily explained. Therefore, the molecular dynamics (hereafter, MD) simulation derived trajectories, and the temporal behaviors of the phenylene rotator in real–time scales would definitely be varied if the MD simulation scheme is run under the "DFTB2+PBC" and "DFTB1+PBC" with and without Slater–Kirkwood model. Based on the same analogies, the temporal dependencies and the comparable real–time flipping motions studies of the phenylene rotator of the siloxaalkane molecular gyroscope were carried out under these two methods separately at wide ranged kinetic temperature regimes as presented in subsection 3.2.

Table 1. The potential energy surfaces (PESs) retrieved angular positions A, B, and C of the phenylene rotator and their 1π –flipped degenerate positions A', B', and C'.

Methods	Dihedral angle ϕ of the stable positions (extracted from the PESs)		
	First $\leftrightarrow 1\pi$ –flipped	Second $\leftrightarrow 1\pi$ –flipped	Third $\leftrightarrow 1\pi$ –flipped
	A \leftrightarrow A'	B \leftrightarrow B'	C \leftrightarrow C'
X–ray	$0.19\pi \leftrightarrow 1.19\pi$	$0.55\pi \leftrightarrow 1.55\pi$	$0.78\pi \leftrightarrow 1.78\pi$
DFTB1 + PBC	$0.05\pi \leftrightarrow 1.05\pi$	$0.35\pi \leftrightarrow 1.35\pi$	$0.76\pi \leftrightarrow 1.76\pi$
DFTB2 + PBC	$0.01\pi \leftrightarrow 1.01\pi$	$0.35\pi \leftrightarrow 1.35\pi$	$0.76\pi \leftrightarrow 1.76\pi$
DFTB2+PBC+"dispersion energy corrections"	$0.01\pi \leftrightarrow 1.01\pi$	$0.35\pi \leftrightarrow 1.35\pi$	$0.70\pi \leftrightarrow 1.70\pi$

Table 2. The PESs derived flipping barriers E_a of the phenylene rotator exist in between its A, B, C and their 1π –flipped A', B', and C' stable positions, and the structural topology dependent free–volume unit.

Methods	Flipping barriers E_a (kcal/mol) between the stable positions						Free–Volume (average) (\AA)		
	C \rightarrow B	B \rightarrow A	C \rightarrow A'	A' \rightarrow B'	B' \rightarrow C'	C' \rightarrow A			
X–ray	–	–	–	–	–	–	3.9	4.3	5.1
DFTB1 + PBC	0.4	0.7	0.1	0.2	0.7	0.1	4.1	4.1	5.2
DFTB2 + PBC	0.2	0.8	0.05	0.2	0.8	0.05	4.1	4.1	5.3
DFTB2 + PBC + "dispersion energy corrections"	0.1	1.2	0.5	0.1	0.9	0.5	4.2	4.3	5.4

3.2 Real-Time Flipping Motions of the Phenylene Rotator

All the rotary dynamics associated datasets (subsection 3.1) retrieved from the respectively derived PESs (Table 1 and 2) are to be validated to the most extent by the temporal behavior of the phenylene rotator. Herewith, the dihedral angle ϕ (π) of the rotator computed from each MD step unit-cell geometry at each specific kinetic temperature T is plotted with the simulation time (ps) (Fig. 1–Fig. 4) in order to investigate its real-time flipping motions, and the closely associated picosecond rotary dynamics. The graphical representations for the time dependent angular variations of the rotator computed from the MD trajectories datasets derived by the DFTB2 and DFTB1 under PBC with and without "dispersion energy corrections" are shown separately at each kinetic temperature; $T = 1200$ K, 800 K, 600 K, and 300 K (These temperatures were selectively chosen here in order to deduce the experimentally unrevealed rotary dynamics at wide ranged temperature regimes, and more particularly, $T = 300$ K was taken mainly to examine whether the rotator flips facilely at energy as equal as room temperature or not). Since, the rotary dynamics linked datasets retrieved from the DFTB1 + PBC derived PES are not much distinctive to those obtained from the DFTB2+PBC derived PES, present author did not run the MD simulation trajectories just under the latter scheme; instead, the Slater–Kirkwood model was incorporated into its parser code, and run several MD trajectories with different initial velocities of the atomic nuclei for the sake of inquiring the most predominant effects of van der Waals type intra- and inter- molecular interactions, and their needfulness of precise addressing/evaluations in simulating the present type giant crystalline molecular assembly dynamically; which in fact was mostly recognized by the present author as a primary credential to improvise the PES, and to make it more accurate yet contrastingly different to that derived through the DFTB1 and DFTB2 under PBC schemes only [17]. In order to mark the flipping

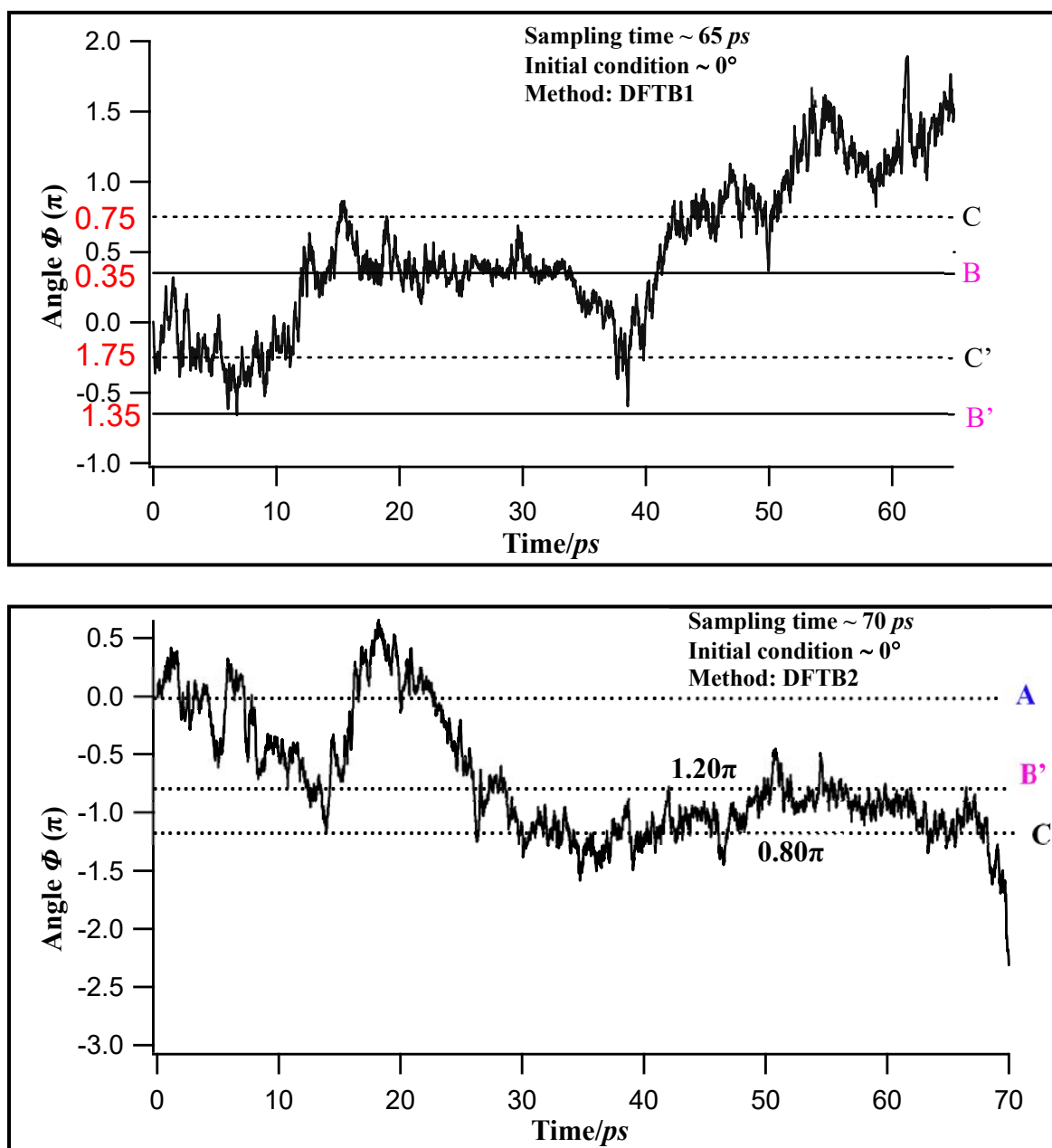


Figure 1. Dihedral angles ϕ of the phenylene rotator as a function of time at 1200 K (a) DFTB1 +PBC (without dispersion energy corrections) (b) DFTB2+PBC (with dispersion energy corrections). The symbols A, B, C, etc. represent stable angular positions of the phenylene rotator.

sites of the phenylene rotator clearly & demonstratively, and to display its correct time-dependent angular positions compatible to those extracted from the PESs (Table 1), the same representations such as A, B, & C for the initial stable positions, and A', B', & C' for the 1π -flipped positions are mentioned on its time-dependent rotary profiles (Fig. 1–Fig. 4) at each kinetic temperature T where the complete MD simulation conditions and the specific method employed to run the same are shown in each inset.

As shown in DFTB1 + PBC derived trajectory pathway at $T = 1200$ K (Fig. 1), the phenylene rotator flips from the original

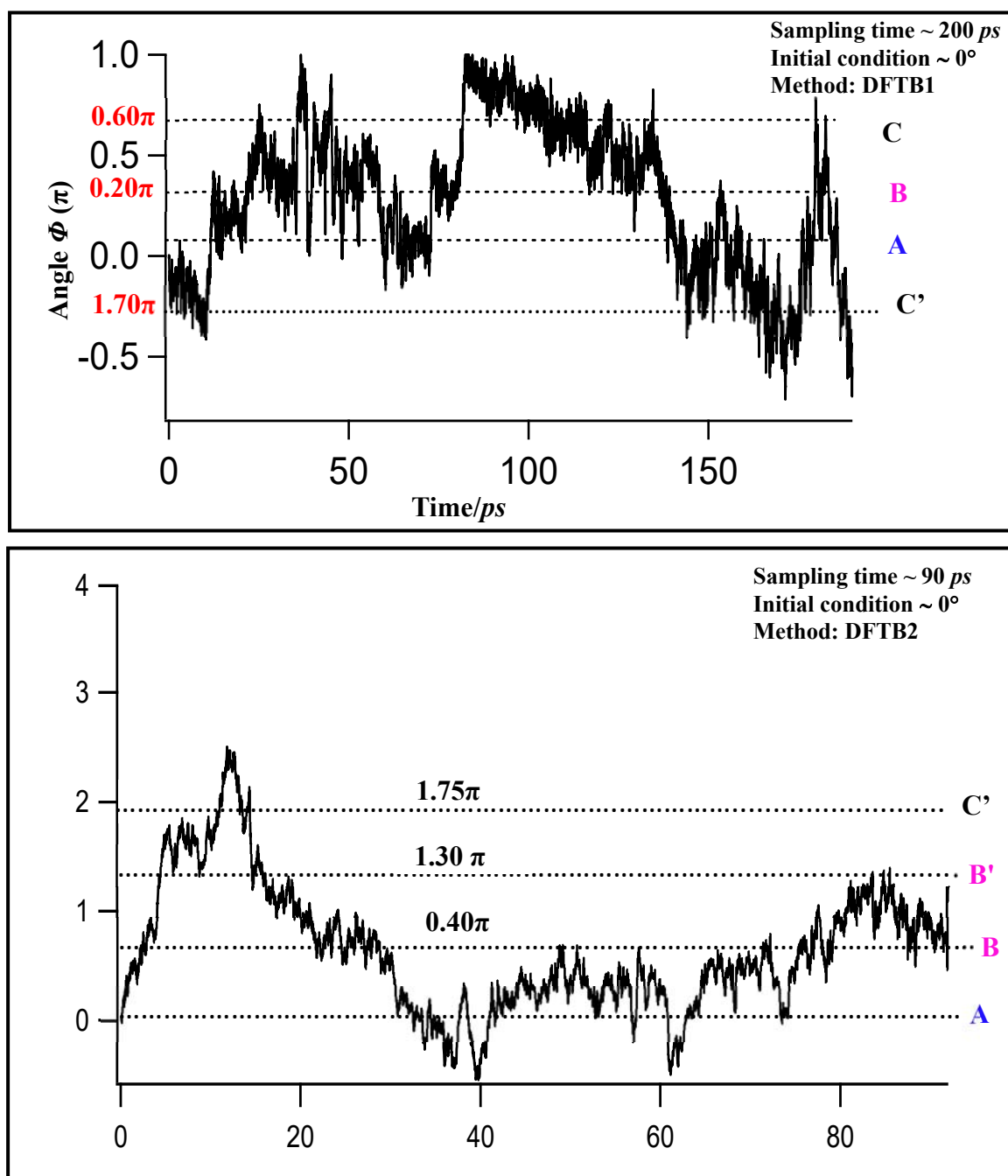


Figure 2. Dihedral angles ϕ of the phenylene rotator as a function of time at 800 K (a) DFTB1 +PBC (without dispersion energy corrections) (b) DFTB2+PBC (with dispersion energy corrections). The symbols A, B, C, etc. represent stable angular positions of the phenylene rotator.

position A to B' via C' followed by its angular switching to the position B mostly. The lifespan of the phenylene rotator on the position C' is appeared as relatively shorter than that on the position B. The approximate time period for it to stay at position B is ~ 30 ps; the longest one than that residing in other stable positions. This observation is not beyond our expectations because the structure B of the molecular gyroscope (with phenylene position B) was predicted as the most stable both by the experimental and

theoretical techniques [13, 17]. After about 2 ps of its stay in position C', the rotator flips to position C where its lifespan is tentatively not less than ~ 10 ps. This real-time flipping motion became recognizably different after implementing "dispersion energy corrections" into the DFTB2 scheme at the same kinetic temperature ($T = 1200$ K). In this case, the phenylene rotator from the original position A flips firstly to position B' shortly followed by its angular switching back to position A. The rotary pathway instantly reaches to the position C where the phenylene rotator stays for about 15 ps. Immediately after this longer stay, it flips to position B' and again remains there for about ~ 25 ps before flipping back to position C. The longest time period observed to occupy at position B' is reasonable here because it is the degenerate position of B; the lowest energy yet most stable position among three. Even though more frequent flipping between the intermittent stable positions are not observed within the framework of currently run MD timescale (~ 70 ps, due to being this simulation computationally expensive and time-consuming), the real-time flipping motion of the specific rotator is genuinely observed at 1200 K under the realistic crystalline condition (PBC + dispersion energy corrections). This is the firstly observed real-time flipping motion of the phenylene rotator of the crystalline siloxaalkane molecular gyroscope at higher temperature scale. The flipping trajectory at 800 K also demonstrates the similar type flipping motions of the phenylene rotator in between its three stable positions. As shown in Fig. 2, the DFTB1 predicted the flipping motion as: a rotator at

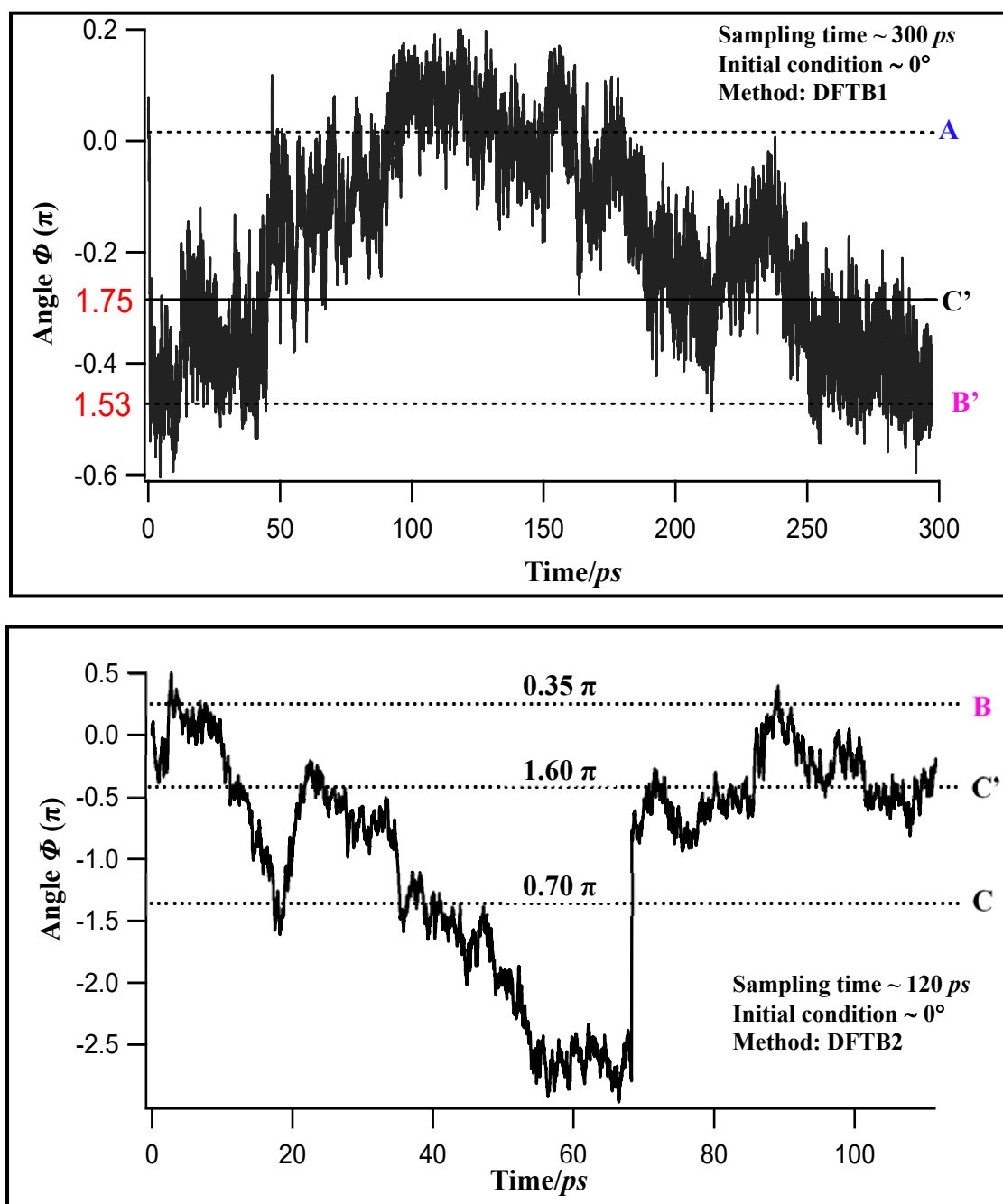


Figure 3. Dihedral angles ϕ of the phenylene rotator as a function of time at 600 K (a) DFTB1 + PBC (without dispersion energy corrections) (b) DFTB2+PBC (with dispersion energy corrections). The symbols A, B, C, etc. represent stable angular positions of the phenylene rotator.

position A flips to C' followed by the longest stayed flipping position B. The average lifetime of the rotator at position B is around

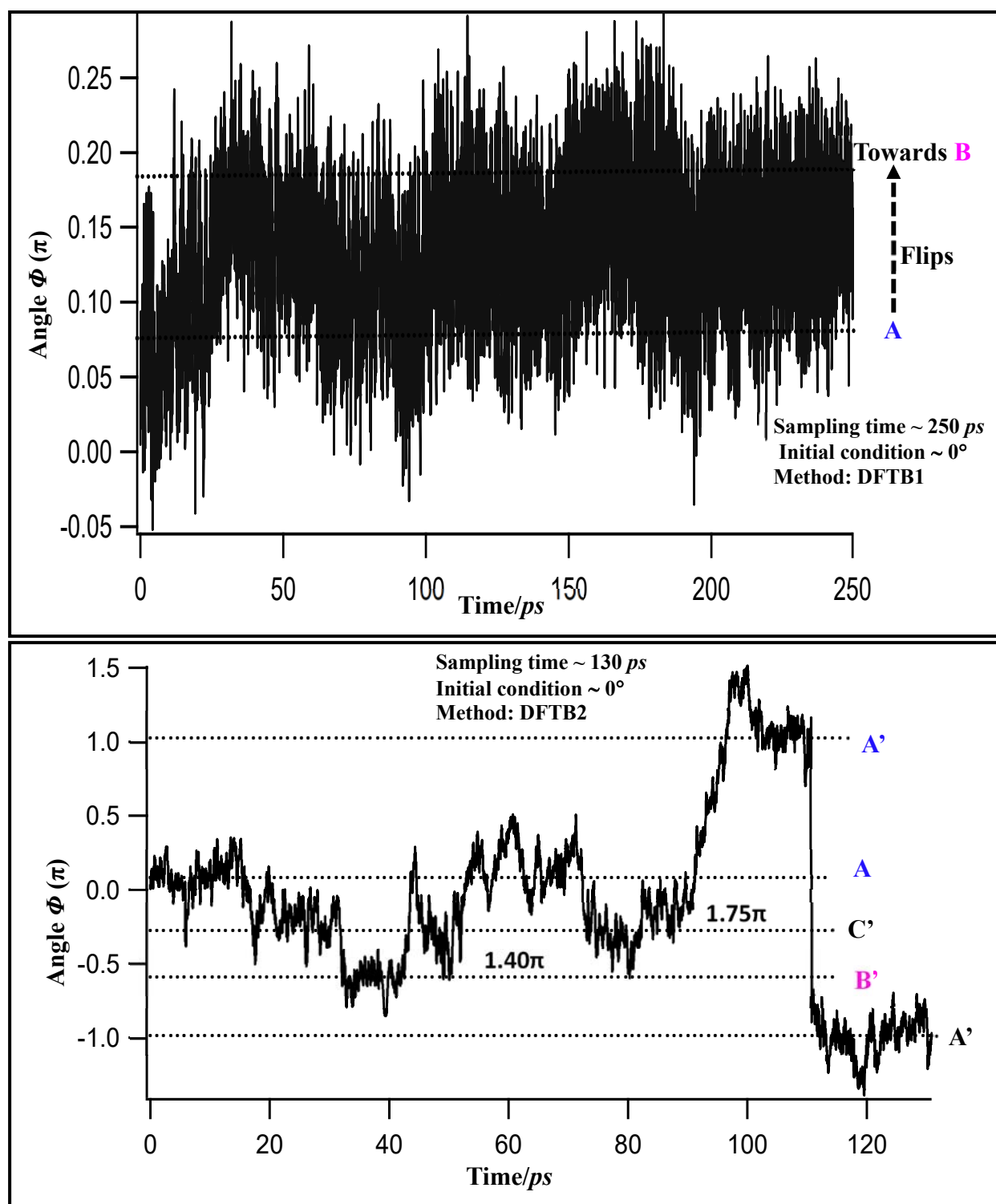


Figure 4. Dihedral angles ϕ of the phenylene rotator as a function of time at 300 K (a) DFTB1+PBC (without dispersion energy corrections) (b) DFTB2+PBC (with dispersion energy corrections). The symbols A, B, C, etc. represent stable angular positions of the phenylene rotator.

~70 ps. After this stay, the phenylene flips from position A to C via B where the rotator consecutively changes its flipping angle

before reaching to C'. At position C', the rotator again remains there for ~ 30 ps to ~ 40 ps before switching its angular position to C. Again, at this temperature scale, the rotator is found to occupy the longest time period at its most stable position B which is as obvious as the observations predicted under the highest temperature $T = 1200$ K. This facile real-time flipping motions of the phenylene rotator are also predicted under "DFTB2+PBC+dispersion energy corrections" schemes. In this case, the phenylene rotator flips from the position A to C' via B', and then reaches to the position B where the rotator remains for about 10 ps before flipping to position A, and again returns back to the most stable position B, and stays there for about 40 ps. The flipping trajectory moves towards position B' from B shortly, and again comes back to B. It indicates that the trajectory as a whole again remains mostly on the periphery of positions B and B' within the current simulation timeframe (~90ps); a quite obvious observation if we consider the stability of these two 1π flipped positions energetically. But, the variations observed in the flipping positions of the rotator and its tentative lifespans in them after imposing "dispersion energy corrections" at the same kinetic temperature T are none other than due to the primary effects of van der Waals type intra- (interactions between the rotator and stator) and inter- (cumulative interactions between the periodically arranged molecular gyroscopes, and their rotating segments and static siloxaalkane arms) molecular interactions exist predominately in the present crystalline molecular gyroscope.

At relatively low kinetic temperature regimes ($T = 600$ K and 300 K), the concerned MD trajectory (Fig. 3 and Fig. 4) leading flipping motions and the rotary dynamics are appeared less frequently with relatively slower rates, which is however very obvious if we consider the internal energy of the ensemble corresponding to that particular temperature regimes. At 600 K, the DFTB1 predicted rotary pathway at first turns into the position B' from the original position A, and proceeds towards the position C' after about 20 ps of its stay at position B'. The pathway then suddenly flips to the position A, and remains there for about 100 ps which then proceeds towards the position C' and B' turn by turn. These real-time flipping motions (though relatively few) are observed even within the MD simulation timescale of ~300 ps; a practically affordable time scales in the framework of current ensemble size and present crystalline molecular arrays plus the directly accessible computational resources. At this temperature, the phenylene flippings to the most stable position B or B' from either of the stable positions are not observed; instead, position A finds easy access and facile flipping pathway towards the position C' (anticlockwise rotation). This is quite logical because the phenylene rotator has to cross taller barrier heights $E_{a1} = 0.3$ kcal/mol (obtained from the PES [17]) associated with A & B (clockwise), and $E_{a2} = 0.2$ kcal/mol associated with C & B (anticlockwise) for undergoing A→B and C→B flippings respectively, and it may need longer time periods to exhibit the same instantly. In other words, the internal energy equivalent to $T = 600$ K kinetic temperature of the present crystalline molecular ensemble is smaller in magnitude than either of the barrier heights E_{a1} & E_{a2} which is in principle not enough to overcome the latter instantly within ~300 ps. The flipping patterns transit to the slightly different directions after incorporating "dispersion energy corrections" features into the DFTB2 scheme. The phenylene rotator from the original position A is found to flip to the position B before reaching to the position C via C'. Again, it moves towards the position C' from C, and remains there for about 15 ps before flipping back to the position C. The phenylene rotary trajectory after 70 ps of the MD run reaches to the position C', and attains there the lifespan of ~ 15 ps. The shortly stayed yet suddenly flipped position B is also noticed along this rotary pathway. Though the frequent flippings of the rotator between its stable positions are not detected, the few flipping motions with shorter lifespans are found to occur even within the framework of current simulation timescale (~ 120 ps) at low temperature regime. It tends to verify the experimentally reported facile phenylene rotations at $T \geq 223$ K. Unlike at $T = 600$ K, the concerned rotary trajectory at $T = 300$ K is found to turn very slowly towards the position B from the original position A progressively even when the MD trajectory was run for relatively longer time scale (~300 ps). Throughout this timeframe, the angular variation of the rotator is noticed just to be around the position A and near to the position B, but not fully flipped to each other. This is however not an abnormal observation based on $T = 300$ K kinetic temperature scale as the internal energy of the ensemble corresponding to that particular T (as equal as room T) is not enough to cross A→B or B→A flippings barriers E_a ; 0.3 kcal/mol and 0.9 kcal/mol [17] respectively. It suggests that the experimentally observed room temperature flipping motions of the phenylene rotator of present molecular gyroscope could be deduced at $T = 300$ K if it was simulated for the longer time scale (> 300 ps) which is, however found impractical. The relatively more subsequent yet progressive type flipping motions of the phenylene rotator in between its experimentally observed intermittent positions are seen across the rotary trajectory path predicted under "DFTB2 + PBC + dispersion energy corrections" scheme at $T = 300$ K. As shown in the concerned diagram (Fig. 4), the rotary trajectory flows constantly for about 18 ps by maintaining an angle designated to the position A, and moves towards the position C' and B' one by one with ~15 ps and ~ 8 ps lifespans in each. The trajectory after ~ 50 ps of the MD run turns towards the position A via C', and remains there for about 25 ps before returning back to C'. The trajectory after 90 ps time period switches to the angular position A' which then flips suddenly to the anticlockwise direction. Despite observing these severe yet actual flipping motions of

the phenylene rotator even at $T = 300$ K after treating the van der Waals dispersion energies under DFTB2+PBC scheme, no principal flipping motions involving the most stable positions B & B' are noticed. This is due to the existence of the tallest rotational energy barrier E_a in between them among other flipping positions, and it would only be crossed fully if the MD simulation timescales at low T were set unexpectedly longer or the internal kinetic energy of the ensemble was increased.

As a whole, the quantum mechanically predicted temporal behaviors of the phenylene rotator at four different kinetic temperatures T depict its facile flipping motions with demonstrative pathways; more particularly at high temperature regimes (1200 K, 800 K, and 600 K). The approximate lifetimes for it to remain at the specific stable angular positions are ranged from sub-pico-seconds to picoseconds. When $T = 1200$ K, the flipping motion of it is more frequent followed by the retardation of the same when T is reduced to 800 K and 600 K. At 800 K, the "DFTB1+PBC" derived MD trajectory shows < 15 ps for the direct 1π phenylene flipping, whereas the "DFTB2 + PBC + dispersion energy corrections" shows > 15 ps; resembling with the facts that the latter scheme predicted much higher rotational energy barriers E_a which actually makes the concerned flipping rate slower. More particularly at $600 \text{ K} \geq T \leq 1200 \text{ K}$, the phenylene rotator is observed to flip between its stable positions at the intervals of several tens of picoseconds, and the entire 1π inversions of the flipping positions are occurred facilely. These MD simulation based results reflect that the phenylene rotator is able enough to cross the energy barriers E_a exist in between any of its two stable positions easily at high kinetic temperatures ($T = 1200$ K and 800 K) (energy of the ensemble). But, when the temperature $T = 300$ K, the MD trajectory tends to demonstrate the flipping motion within the current simulation time scale (300 ps), but is not found to be aligned fully to the angular positions of A, B, or C; suggesting the need of longer simulation time scale (> 300 ps) which is, however beyond the limit of practically affordable computational steps. In this case, exhibiting 1π inversion type rotation of the phenylene rotator in the picosecond regime strongly depends on the initial velocities of the atomic nuclei. It ultimately ensures us that the current MD simulation time-scale framework is not enough for the phenylene rotator to overcome any sorts of the barriers (Table 2) exist in between any of its stable positions A, B, & C (and their 1π -flipped positions). More apparently, the relatively more demonstrative yet longer lifespans occupying flipping motions of the rotator are observed at both high and low temperature regimes while employing the DFTB2+PBC scheme with "dispersion energy corrections" features. It thus guaranties that the predominant effects of the van der Waals dispersions and the related long-ranged interactions exist in the present type crystalline molecular assemblies has to be addressed properly with the effective quantum mechanical parametrizations in order to make the current type NVE simulating systems realistic yet consistent to the solid state materials. All these splendid real-time observations of the phenylene flipping motions, and the closely associated theoretical interpretations concentrated into the amphidynamic type crystalline molecular solid ensure us that the DFTB⁺ simulation package does host many potential mathematical formulations that not only offers an exceptional computing ability and the remarkable long-ranged non-bonding type interactions treating quantum mechanical skills but also allows the chemists to simulate even the giant crystalline systems two order of magnitudes faster than the rate offered by the typical density functional theory DFT; a very promising prerequisites of the solid state systems' simulation package and the gigantic molecular assemblies' modeling simulation environment.

3.3 Validations of the Rotational Energy Barriers E_a from Real-Time Flipping Dynamics

In dynamical studies, the Arrhenius equation is always regarded as an important mathematical tool in order to estimate the activation energy barrier E_a (in this case, flipping barrier E_a) quantitatively. Mathematically, it is the logarithmic expressions that relate the rate constant κ (in this case, flipping rate of the phenylene rotator) with E_a and associated temperature T in absolute scale (in Kelvin) as shown in eq. (1) and eq. (2).

$$\kappa = A e^{\frac{-E_a}{K_B T}} \quad (1)$$

$$\ln \kappa = \ln A - \frac{E_a}{K_B T} \quad (2)$$

Where;

A = pre-exponential factor, and

K_B = Boltzmann constant (1.987×10^{-3} kcal mol⁻¹ K⁻¹).

In the current "DFTB1+PBC"/MD and "DFTB2+PBC+dispersion energy corrections"/MD simulations, the facile real-time flipping motions of the phenylene rotator of the siloxaalkane molecular gyroscope (subsection 3.2) are observed mostly

at high kinetic temperature regimes ($T = 800$ K and $T = 1200$ K). Therefore, the average flipping rates of it from the stable positions B to A (B→A) at the respective absolute temperature scales are calculated as (a) "DFTB1+PBC" method: $\kappa_1 = 0.018$ ps⁻¹ and $\kappa_2 = 0.021$ ps⁻¹; (b) "DFTB2+PBC+dispersion energy corrections" method: $\kappa_1 = 0.009$ ps⁻¹ and $\kappa_2 = 0.013$ ps⁻¹. In both of the methods, the rate of the phenylene flipping motion increases in the same range while increasing the internal kinetic temperature T of the ensemble to 1200 K from 800 K. It is an obvious observation in terms of the externally provided temperature components of the simulating atomic nuclei of the ensembles, and their respective internal energies involved in inducing the phenylene ring to rotate facilely at higher temperature scale (subsection 3.2). And, the rotational rates κ of the phenylene rotator are predicted as slower (time consuming) at the same kinetic temperature T after incorporating the van der Waals type "dispersion energy corrections" features (in this case, Slater–Kirkwood model) into the DFTB2 scheme. It confirms that there is a presence of taller energy barrier E_a , and more time consuming rotary pathway in between the flipping positions B and A, and it is very obvious if we refer to the respectively derived PESs [17]. It further ensures us that the van der Waals interactions do create substantial contributions which in fact involves directly in surpassing the rotational energy barrier E_a by about ~ 0.4 kcal/mol, and thus, make the rotary motion significantly slower.

In order to validate the *Gaussian–external* methodology drove DFTB methods derived PESs extracted E_a values for the particular phenylene B→A flipping, the Arrhenius equation (eq. 2) is presented explicitly here at two different kinetic temperatures $T_1 = 800$ K and $T_2 = 1200$ K, and the corresponding two different flipping rates κ_1 and κ_2 as; eq. (3) and eq. (4) before integrating them into a single equation (eq. (5)).

$$\ln \kappa_1 = \ln A - \frac{E_a}{k_B T_1} \quad (3)$$

$$\ln \kappa_2 = \ln A - \frac{E_a}{k_B T_2} \quad (4)$$

After rearranging the eq. (4), and substituting the value of $\ln A$ to eq. (3), the final pre-exponential factor A eliminated form of the Arrhenius equation is achieved as shown in eq. (5).

$$\ln \left[\frac{\kappa_1}{\kappa_2} \right] = - \frac{E_a}{k_B} \left[\frac{1}{T_1} - \frac{1}{T_2} \right] \quad (5)$$

After substituting the respective absolute temperatures T_1 & T_2 , and the corresponding MD trajectories derived flipping rates κ_1 and κ_2 in eq. 5, the energy barrier E_a for exhibiting B to A flipping (B→A) is estimated as; (a) for "DFTB1+PBC": $E_a = 0.66$ kcal/mol, and (b) for "DFTB2 + PBC+dispersion energy corrections": $E_a = 1.84$ kcal/mol respectively. The corresponding values appeared at the respectively derived PESs for the same B→A flipping are 0.70 kcal/mol and 1.2 kcal/mol respectively [17]. These respective E_a values estimated through the DFTB based MD simulations and the *Gaussian–external* based PES scanning techniques are in quite agreeable range if we realize the complexity of the present simulating crystalline molecular assemblies and the most rigorous long-ranged interactions treating mathematical formulations of the DFTB⁺.

IV. CONCLUSIONS

The present research work was mainly aimed at studying real-time flipping motions of the phenylene rotator encapsulated into the Si–C bond spin axis linked –Si– & –Si–O– made siloxaalkane framework of the crystalline molecular gyroscope. As per the X-ray and ¹H–NMR based experimental observations, this siloxaalkane molecular gyroscope was found to behave as an amphidynamic crystalline material: the phenylene rotator was observed to flip facilely along its spin axis among three stable positions designated as A, B, and C, and their corresponding 1π -flipped degenerate positions A', B', and C' at temperature $T \geq 223$ K while the peripheral siloxaalkane framework remains fully static yet flexible. Owing these amphidynamical features plus many other promising physicochemical properties of this molecular gyroscope functionalizable to nanotechnology and molecular machinery, series of the experimental and theoretical research works concentrated into its crystal structures, molecular energetics, rotary dynamics, and mostly the external–stimuli controlled internal rotations were already reported by many prominent authors. Amidst these research works and exceptional experimental & theoretical findings, none of the contributions were found to theorize fully the experimentally unpredicted yet impossible type real-time flipping motions and the temporal behavior of its phenylene rotator under the complete crystalline conditions (periodic boundary condition PBC, and van der Waals type "dispersion energy corrections"). With this regarded as a major motivation for the present work, the theoretically renowned self-consistent (SCC) and non-self-consistent charge (NCC) based density-functional tight-binding schemes, respectively called DFTB2 and DFTB1, were

applied explicitly to this specific molecular gyroscope under PBC with and without "dispersion energy corrections" features, and the respective molecular dynamics (MD) simulations formulations were implemented at wide ranged kinetic temperature regimes; $T = 1200$ K, 800 K, 600 K, and 300 K for the practically reasonable timescales. The designated dihedral angle ϕ of the phenylene rotator in respect to the static siloxaalkane arm representing its exact angular position (rotary positions) centrally was determined for each MD step recurring unit–cell geometry, and the concerned rotary trajectory pathway at each T was sketched as a function of time in picosecond regime. Based on the similar theoretical methods predicted potential energy surfaces (PESs) associated rotary parameters such as flipping energy barriers E_a , clockwise and anticlockwise 1π inversions, and the structural topology dependent free–volume units, the concerned rotary trajectories derived at each specific T were analyzed quantitatively from which the picosecond rotary dynamics of the phenylene rotator was retrieved in real–time scales. The general results as a whole were found to demonstrate the experimentally observed flipping motions of the phenylene rotator along with depicting several intermittent and 1π inversion type flipping genuinely.

More particularly, at high kinetic temperature regimes ($T = 1200$ K, 800 K, and 600 K), the complete 1π inversions of the phenylene rotator were observed facily, and the approximate lifetimes for it to remain at the specific stable angular positions were found to range from sub– picoseconds to picoseconds. When $T = 1200$ K, the flipping motion of the rotator was more frequent followed by the retardation of the same when T was reduced to 800 K and 600 K each. More apparently, when the DFTB method was switched from "DFTB1+PBC" to "DFTB2 + PBC + dispersion energy corrections", the time required to exhibit several intermittent flipping motions of the phenylene rotator between its designated stable positions A, B, C, A', B', & C', and the complete 1π inversion flipping was quite distinctive. For example, at $T = 800$ K, the former method predicted less than 15 ps time period for 1π inversion type flipping, whereas the latter predicted more than 15 ps for the same. When $T = 600$ K, the phenylene rotator was observed to flip between its stable positions at the intervals of several tens of picoseconds. But, when T was decreased to the scale of room temperature ($T = 300$ K), the former method derived MD trajectory was found to be tended progressively towards the path of showing A to B phenylene flipping even within the 300 ps simulation time scale, however, it was unable to reach fully into the stable position B. It means the phenylene rotator was not found to overcome any sorts of its energy barriers E_a exist in between the stable positions A, B, & C (and their 1π –flipped positions) at $T = 300$ K. It ultimately reflected us to project here that the current MD simulation time–scale adopted for simulating the present molecular gyroscope at $T = 300$ K was not enough. However, the relatively more demonstrative, experimentally more compatible yet longer lifespans occupying flipping motions of the phenylene rotator were recorded at both high and low temperature regimes while employing "DFTB2 + PBC + dispersion energy corrections" scheme. Beside this, the phenylene rotator position B to A (B→A) flipping rates $\kappa_1 = 0.018$ ps⁻¹ & $\kappa_2 = 0.021$ ps⁻¹ predicted by the DFTB1 at $T = 800$ K & 1200 K respectively were contrastingly different in magnitudes to those predicted by the DFTB2 as $\kappa_1 = 0.009$ ps⁻¹ and $\kappa_2 = 0.013$ ps⁻¹. And, the Arrhenius equation based B→A flipping barriers computed from these respectively derived κ datasets were $E_{a1} = 0.66$ kcal/mol, and $E_{a2} = 1.84$ kcal/mol respectively; the quite agreeable E_a values to those retrieved from the respectively generated PESs: $E_{a1} = 0.70$ kcal/mol & $E_{a2} = 1.2$ kcal/mol. All these MD simulations based quantitative interpretations and theoretical predictions assured us to underscore the significance of incorporating van der Waals dispersions and the related long–ranged molecular interactions treating mathematical formulations into the quantum mechanical parametrizations of the simulation package in order to assume the NVE ensemble realistically yet consistently under the complete requirements of solid state systems. And, the exceptional performances of the "dispersion energy corrections" addressing Slater–Kirkwood model adopted DFTB2/MD scheme promoted itself as a standalone quantum mechanical applications in the view of not only offering outstanding computing abilities but also guarantying to undertake the giant crystalline molecular assemblies rationally with two order of magnitudes faster computational parser codes relative to that for the typical density functional theory.

V. ACKNOWLEDGEMENT

The entire real–time flipping motions and the associated picosecond flipping dynamics of the phenylene rotator of the crystalline siloxaalkane molecular gyroscope presented throughout this research article were based on the calculations carried out with the high performance computing systems available at Theoretical Chemistry Laboratory, Graduate School of Science, Tohoku University, Sendai, Miyagi, Japan.

COMPETING INTERESTS

Author has declared that no competing interests exist.

REFERENCES

- [1] Seifert G. Tight-Binding Density Functional Theory: An Approximate Kohn–Sham DFT Scheme. *Journal of Physical Chemistry A*. 2007; 111:5609–5613.
Available: <https://pubs.acs.org/doi/10.1021/jp069056r#:~:text=The%20DFTB%20method%20is%20an,and%20to%20the%20Harris%20functional>.
- [2] Elstner M, Porezag D, Jungnickel G, Elsner J, Haugk M, Frauenheim T, Suhai S, Seifert G. Self-consistent-charge density-functional tight-binding method for simulations of complex materials properties. *Physical Review B*. 1998; 58:7260–7268.
Available: <https://journals.aps.org/prb/abstract/10.1103/PhysRevB.58.7260>
- [3] Aradi B, Hourahine B, Frauenheim T. DFTB+, a Sparse Matrix-Based Implementation of the DFTB Method. *Journal of Physical Chemistry A*. 2007; 111:5678–5684.
Available: <https://pubs.acs.org/doi/10.1021/jp070186p#:~:text=The%20sparsity%20is%20calculated%20as,unique%20among%20current%20DFTB%20implementations>.
- [4] Elstner M, Frauenheim T, Kaxiras E, Seifert G, Suhai S. A Self-Consistent Charge Density-Functional Based Tight-Binding Scheme for Large Biomolecules. *Physica Status Solidi B*. 2000; 217:357–376.
Available: [https://onlinelibrary.wiley.com/doi/10.1002/\(SICI\)1521-3951\(200001\)217:1%3C41::AID-PSSB41%3E3.0.CO;2-V](https://onlinelibrary.wiley.com/doi/10.1002/(SICI)1521-3951(200001)217:1%3C41::AID-PSSB41%3E3.0.CO;2-V)
- [5] Frauenheim T, Seifert G, Elstner M, Niehaus T, Kohler C, Amkreutz M, Sternberg M, Hajnal Z, Di Carlo A, Suhai S. Atomistic simulations of complex materials: groundstate and excited-state properties. *Journal of Physics Condensed Matter*. 2002; 14(11):3015–3047.
Available: <https://iopscience.iop.org/article/10.1088/0953-8984/14/11/313/meta>
- [6] Marahatta AB. Performance Evaluation of DFTB1 and DFTB2 Methods in reference to the Crystal Structures and Molecular Energetics of Siloxaalkane Molecular Compass. *International Journal of Progressive Sciences and Technologies*. 2023; 41(1):12–31.
- [7] Marahatta AB, Kono H. Performance of NCC- And SCC- DFTB Methods for Geometries and Energies of Crystalline Molecular Gyroscope. *International Journal of Innovative Research and Advanced Studies*. 2019; 6(5):180–185.
Available: http://www.ijiras.com/2019/Vol_6-Issue_5/paper_28.pdf
- [8] Zheng G, Irle S, Morokuma K. Performance of the DFTB method in comparison to DFT and semiempirical methods for geometries and energies of C₂₀–C₈₆ fullerene isomers. *Chemical Physics Letter*. 2005; 412: 210–216.
Available: <https://www.sciencedirect.com/science/article/abs/pii/S0009261405009334>
- [9] Ohta Y, Okamoto Y, Irle S, Morokuma K. Single-walled carbon nanotube growth from a cap fragment on an iron nanoparticle: Density-functional tight-binding molecular dynamics simulations. *Physical Review B*. 2009; 79:195415 (1–7).
Available: <https://journals.aps.org/prb/abstract/10.1103/PhysRevB.79.195415>
- [10] Lee KH, Schnupf U, Sumpter BG, and Irle S. Performance of Density-Functional Tight-Binding in Comparison to Ab Initio and First-Principles Methods for Isomer Geometries and Energies of Glucose Epimers in Vacuo and Solution. *American Chemical Society Omega*. 2018; 3(12):16899–16915.
Available: <https://www.ncbi.nlm.nih.gov/pmc/articles/PMC6643604/#:~:text=On%20the%20basis%20of%20a,hydrogen%20bonds%20and%20isomer%20energies>.
- [11] Pekka Koskinen, Ville Mäkinen. Density-functional tight-binding for beginners. *Computational Materials Science*. 2009; 47:237–253.
Available: <https://www.sciencedirect.com/science/article/abs/pii/S0927025609003036>

- [12] D. Frenkel, B. Smit. Understanding molecular simulation, From Algorithms to Applications, Academic Press, 2002.
Available: <https://www.sciencedirect.com/book/9780122673511/understanding-molecular-simulation>
- [13] Setaka W, Ohmizu S, Kabuto C, Kira, MA. Molecular Gyroscope Having Phenylene Rotator Encased in Three-spoke Silicon-based Stator. Chemistry Letters. 2007; 36(8):1076–1077.
Available: <https://www.journal.csj.jp/doi/epdf/10.1246/cl.2007.1076>
- [14] Setaka W, Ohmizu S, Kabuto C, Kira M. Molecular Gyroscope Having a Halogen-substituted p-Phenylene Rotator and Silaalkane Chain Stators. Chemistry Letter. 2010; 39(5):468–469.
Available: <https://www.journal.csj.jp/doi/pdf/10.1246/cl.2010.468>
- [15] Setaka W, Yamaguchi K. Thermal modulation of birefringence observed in a crystalline molecular gyrotop. Proceedings of the National Academy of Sciences of the USA. 2012; 109:9271–9275.
Available: <https://www.pnas.org/doi/10.1073/pnas.1114733109>
- [16] Michl J, Charles E, Sykes H. Molecular Rotors and Motors: Recent Advances and Future Challenges. American Chemical Society Nano. 2009; 3(5):1042–1048
Available: <https://pubs.acs.org/doi/10.1021/nn900411n>
- [17] Marahatta AB, Kanno M, Hoki K, Setaka W, Irle S, Kono H. Theoretical Investigation of the Structures and Dynamics of Crystalline Molecular Gyroscopes. Journal of Physical Chemistry C. 2012; 116:24845–24854.
Available: <https://pubs.acs.org/doi/10.1021/jp308974j>
- [18] Marahatta AB. *Gaussian–External* Methodology Predicted Crystal Structures, Molecular Energetics, and Potential Energy Surface of the Crystalline Molecular Compass. Asian Journal of Applied Chemistry Research. 2023; 14(1):8–25.
Available: <https://journalajacr.com/index.php/AJACR/article/view/255>
- [19] Marahatta AB, Kono H. SCC–DFTB Study for the Structural Analysis of Crystalline Molecular Compasses. Chemistry Research Journal. 2022; 7(4):77–94.
Available: <https://chemrj.org/download/vol-7-iss-4-2022/chemrj-2022-07-04-77-94.pdf>
- [20] Marahatta AB, Kono H. Structural Characterization of Isolated Siloxaalkane Molecular Gyroscopes via DFTB-based Quantum Mechanical Model. International Journal of Progressive Sciences and Technologies. 2021; 26(1):526–541.
Available: <https://ijpsat.org/index.php/ijpsat/article/view/2950/0>
- [21] Marahatta AB, Kono H. Comparative Theoretical Study on the Electronic Structures of the Isolated Molecular Gyroscopes with Polar and Nonpolar Phenylene Rotator. International Journal of Progressive Sciences and Technologies. 2020; 20(1):109–122.
Available: <https://ijpsat.org/index.php/ijpsat/article/view/1716>
- [22] Macrae CF, Edgington PR, McCabe P, Pidcock E, Shields GP, Taylor R, Towler M, van de Streek J. Mercury: visualization and analysis of crystal structures. Journal of Applied Crystallography. 2006; 39:453–457.
Available: <https://onlinelibrary.wiley.com/doi/abs/10.1107/S002188980600731X>
- [23] (a) Verlet L. Computer “Experiments” on Classical Fluids. I. Thermodynamical Properties of Lennard-Jones Molecules. Physical Review. 1967; 159:98–103.

Available: <https://journals.aps.org/pr/pdf/10.1103/PhysRev.159.98>

(b) Verlet L. Computer “Experiments” on Classical Fluids. II. Equilibrium Correlation Functions. Physical Review. 1968; 165:201:214

Available: <https://journals.aps.org/pr/abstract/10.1103/PhysRev.165.201>

[24] DFTB+ Version 1.3 User Manual.

Available: <https://dftbplus.org/fileadmin/DFTB-Plus/public/dftb/current/manual.pdf>